Ex-vessel delayed neutron detection systems for the ASTRID Sodium-cooled Fast Reactor

Romain Coulon, Emmanuel Rohée, Jonathan Dumazert, Sara Garti, Philippe Filliatre, Christian Jammes

Ex-Vessel Delayed Neutron Detection Systems for Sodium Cooled Fast Reactors. Some perspectives for the ASTRID reactors.

Romain Coulon, Emmanuel Rohée, Jonathan Dumazert, Sara Garti, Hassen Hamrita, Philippe Filliatre, Christian Jammes

***Abstract* – Monitoring fuel integrity during sodium cooled fast reactor operating is a particular issue when sodium uranoplutonate formed consecutively to a clad aperture will fostered cooling defaults. Delayed neutron detection systems are key tools allowing preventing and mitigating such an accident by monitoring the concentration of delayed neutron precursors contained into the coolant. DND systems operate in hard gamma rays flux and low neutron activity level. They have to be carefully optimized in order to detect as early as possible dangerous failures. A discussion has been conducted about the best way to design a DND system and some conclusions have been obtained.**

***Index Terms*— Fast reactor; Sodium; Fuel failure; Fission products; Neutron detection.**

I. Introduction

SAFETY is an essential requirement for future Nuclear Power Plant (NPP) projects. Chernobyl, Tree Miles Island, and Fukushima are unforgivable catastrophes for the electronuclear industry. On the other side, electricity needs will increase (industrialization, electrical vehicle development…) and less dangerous zeros carbon energies will reasonably be not able to fully compensate the nuclear part [1]. It is a duty for research institutes to propose NPP projects which will show profitability while including dismantling, nonproliferation, sustainability, long term actinides burning, and moreover **a new grad of safety** [2].

The French Atomic Energy Commission (CEA), works on the development of a Sodium cooled Fast Reactor (SFR) named **ASTRID** "Advanced Sodium Technological Reactor for Industrial Demonstration" [3]. SFR is the most credible technology among GEN.IV candidates, already having a large feedback by many prototypes built worldwide, working as a breeder and potentially allowing closing the fuel cycle. One key part of safety management in ASTRID is the monitoring of the first containment barrier ensured by the fuel pin cladding. The process of fuel failure can be divided in two steps:

R. Coulon, E. Rohée, J. Dumazert, and S. Garti are with the CEA, LIST, F-91191 Gif-sur-Yvette, France. (e-mail: romain.coulon@cea.fr ; phone: +33169088491).

P. Filliatre and C. Jammes are with the CEA, DEN, F-13108 Saint-Paul-les-Durance, France. (e-mail: christian.jammes@cea.fr ; phone: +33442253926).

The first step is named "**gaseous failure**". When a thin failure appears, a burst of noble gas (xenon and krypton) is released into the coolant. Then, at pressure equilibrium between fuel gas and sodium, noble gas fission products are released continuously according to the diffusion process into the fuel. This default is not considered as a safety accident but concerned assembly has to be localized and potential aggravations monitored. Gamma spectrometry systems are used to perform an online analysis of the gaseous fission products contained into the coolant. Currently, works are under investigation to improve the performance of such gamma spectrometry systems [4-6].

The second step is named "**opened failure**". If the failure becomes large enough, sodium can penetrate into the fuel pin. The Reaction between fuel Oxide and Sodium (ROS) induces a chemical reaction producing sodium uranoplutonate $Na_3(U,Pu)O_4$. This complex pumps oxygen from the fuel oxide, and locally decreases the thermal conductivity. Moreover, because its density is two times lower than $(U,Pu)O_2$, the fuel volume is increased enlarging the aperture size [7]. This type of failure is critical and, if not manage quickly, could degenerate blocking the sodium and inducing a cooling default. Opened failure detection systems have therefore to be carefully developed in the framework of future SFR projects, in order to detect as early as possible these dangerous failures. It should be noted that, in this type of failure, fission products are mainly released directly into the coolant by recoil consequently to fission reactions occurring on the periphery of the fuel [8]. On contrary to gaseous failure, halogen fission products as bromine or iodine are released. Among these halogen fission products, some of them are delayed neutron precursors as ^{137}I, ^{87}Br or ^{88}Br and their presence in sodium is therefore a specific signature of opened failure.

Delayed Neutron Detection systems (DND) are apparatus ensuring an online measurement of the neutron activity contained into the sodium coolant.

II. State of the Art

DND systems have been developed and commissioned since the early SFR prototypes. They are installed in the

proximity of hot sodium loops in the case of loop type reactors as for instance the Indian FBTR, the U.S. FFTF, the Japanese Joyo and Monju [9-11]. For pool type reactors, the sodium is sampled though pipes inserted into the hot pool circulating using electromagnetic pumps. This sampling method is the most implemented in SFR reactors allowing a pre-localization of defective assemblies. For instance, the pipe sampling at the French Superphenix allows the division of the core in 6 parts [12-13]. A fine localization approach has been implemented in Phenix and Superphenix and consists to sample, during operation, the sodium at the outlet of each (or per three) fuel assembly. The sodium is mixed or focused using a rotating selector [12]. Others reactors localizes defected assembly after shutdown by dry or wet sipping or during operation by implementing tagging gas into fuel pins (Joyo and Monju) followed by mass spectroscopy analysis [11].

The detection part of the system is thermally isolated from the hot sodium using insulation material and forced nitrogen circulation. Then, a gamma ray shield is set to limit the production of photon pile-up pulses and photoneutron events. Finally, a polyethylene or polypropylene moderator is used to thermalize neutron, increasing the detection sensitivity of neutron detectors those can be: ^{3}He, boron coated or BF_3 proportional counters. Fig. 1 illustrates a standard schematic of a DND system in the case of sampling in pool type SFR.

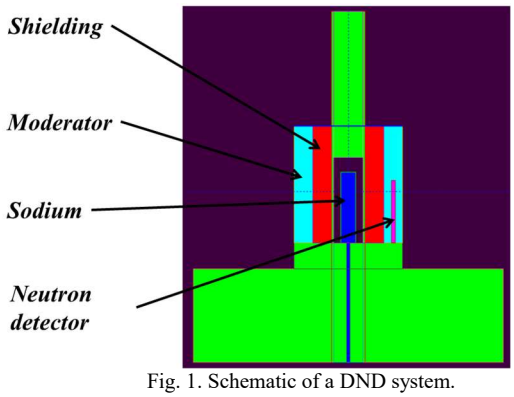

Fig. 1. Schematic of a DND system.

Count per second per square centimeter recoil (cps/cm².R) is a theoretical unit describing the sensitivity of a DND system. It provides the count rate measured by the system for a given aperture area and therefore allows a rough calibration of the system to estimate the area of the failure. This sensitivity gives an order of magnitude of the sensitivity but cannot be considered as fine metrological information. Indeed, the model built to calculate this sensitivity makes the assumption that delayed neutron fission products are only released by recoil whereas they could also be released by diffusion and knock-out mechanisms [13]. Moreover, it is illusory trying to achieve a strong calibration of DND systems because of the number of unpredictable data required by the model as the local fission rate, the local temperature, the local diffusion coefficient, sodium flow rate, etc.

The feedback from operating has highlighted the efficiency of DND systems to detect opened failure with a sufficient earliness. At least 4 open failures have been detected and quickly localized during Phenix operation maintaining the reactor free of any fuel particles into the sodium [14].

In the absence of any failure, a baseline signal is observed due to the pollution of fuel claddings by fissile materials deposited on cladding and by photoneutrons produced by (γ,n) reactions on deuterium nuclei. This baseline will impose the detection limit of the system and its correlation with the power level and other parameters is a problem [15]. Any reduction of this baseline will induce a gain in failure detection performance while maximizing the reactor availability (false alarm reduction).

Alternative techniques have been studied whereby an *in situ* measurement of the delayed neutrons activity is performed. For instance, ionizing fission chambers are set around the vessel of BN600 and BN800 Russian reactors measuring delayed neutron signal from the sodium located behind each intermediate heat exchangers. They allow detecting and locating with a short response time, about 20 s, fuel failures [16]. It can also be noted that high temperature fission chambers are investigated for the ASTRID reactor to be installed *in vessel* [17]. This approach has the advantage to reduce to response time with a very short sodium transit time from fuel to detector (≈ 6 s), to be intrinsically blind to gamma rays thanks to the very high Q-value of the fission reaction, and to suppress photoneutron problem. However, the detection sensitivity decreases compared to those obtained in remote configuration implementing proportional counters; and shielding against core neutron, which will constitute a significant baseline, constitutes a new challenge. In this particular condition, where the neutron baseline can change as a function of the reactor operating parameters, specific algorithms have been developed to manage this effect avoiding false alarms while maintaining good detection efficiency [15,19-21].

In the traditional “ex-vessel” configuration which is by conception free of core neutrons, works have also been carried on the use of an alternative moderator, in order to suppress the photoneutron part of the baseline signal [18]. The graphite moderator is a promising candidate suppressing the photoneutron baseline while suffering a limited sensitivity reduction compared to polyethylene.

III. Specifications

The ex-vessel DND system has to fit with following specifications:

- To be compliant with the **sampling system** and **space limitation** on the reactor floor. The sodium volume of each DND system circulates into a cylindrical container of 5.2 liters with a diameter equal to 86 mm and a height equal to 450 mm. This container is itself encapsulated into steel hood with a diameter equal to 220 mm. The surface available on the reactor floor is a disc with a diameter equal to 700 mm.

- To insulate the detector against **sodium temperature**. The steel hood is filled with thermal insulator (mineral wool) in where heat is removed by nitrogen gas circulation.
- To protect neutron detector against the **gamma flux** emitted by activation products contained into the sodium. A gamma shield is set around the steel hood. Its required thickness depends on the detector technology.
- To limit or suppress all **interference neutrons** production. Photoneutrons have been identified in previews reactors as a significant source of interference neutrons. The gamma ray shielding and moderator have to be conceived according to this requirement. Interference neutrons from cladding contamination with fissile materials are also significant but DND design options cannot play any roles for the reduction of these interferences.
- In order to detect and monitor failure as efficiently as possible, **detector response** to delayed neutrons from fission products has to be maximized. The choice of the detector and its implementation into the system has therefore to be carefully considered.
- Finally, if the system will be installed in an area where operators can work during operation, the limitation of the external dose rate is also an issue.

To study the conception of an ex-vessel DND system for ASTRID reactor, options about detector technology, gamma ray shielding, and moderator, have to be identified.

Due to the high gamma dose rate, we can reasonably focus the study on gas detectors exhibiting high neutron vs gamma discrimination rate. They can be:

- ^{3}He proportional counters,
- ^{10}B proportional counters,
- Or ionizing fission chambers.

It must be noted here that, inorganic or organic scintillators become ineffective in dose rates above 10 mGy.h^{-1}. Small semi-conductors technologies, such as SiC, diamond or CdZnTe, covered or doped with neutron convertors [22-24], enable neutron detection in a relatively high gamma dose rate, but their low geometrical efficiency disagree with the requirement of neutron sensitivity maximization.

Gamma ray shielding are usually based on lead or tungsten, both having high atomic number (Z_W=74 and Z_{Pb}=82) and high density (ρ_w=19.3 g.cm-^{3} and ρ_{Pb}=11.35 g.cm^{-3}).

The best material used for neutron moderation is the High Density PolyEthylene (HDPE) providing a high concentration of hydrogen nuclei. Because of the photoneutron issue, a moderator with small atomic number and without hydrogen has to be envisaged. The graphite will be therefore a part of this study.

IV. Calibration of the Model

To discus DND systems conception, a digital model of the system is built. MCNP6 is used as a validated code to simulate by Monte-Carlo method the transport of neutron and gamma particles.

Detectors are chosen within the industrial catalogues with a length close to those of the sodium container (≈ 450 mm). Three models of detector are considered in this study:

- A ^{3}He proportional counter 65NH45 (Mirion Canberra),
- A ^{10}B proportional counter CPNB48 (Photonis),
- An ionizing fission chamber CFUC07 (Photonis).

Proportional counters CPNB48 and 65NH45 are set into a HDPE bloc covered with cadmium in order to suppress the signal from neutrons moderated outside. Fig. 2 shows the MCNP6 geometry of the bloc and the location where counters are inserted. Counters are linked to NIM units MIRION Canberra 7820 and 7821 used to supply voltage, amplified and filtered the signal. A ^{252}Cf neutron source with an activity equal to 710 kBq is used to perform 12 measures divided in 2 sets (each side) of 6 points separated to each other by a 10 cm step.

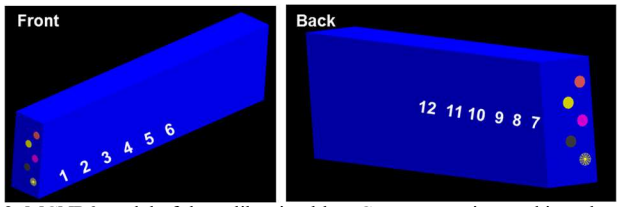

Fig. 2. MCNP6 model of the calibration bloc. Counters are inserted into the central hole (in pink).

MCNP6 has the capability to generate and transport charges ions from neutron captures ^{10}B(n,α)^{7}Li and ^{3}He(n,p)^{3}H [25]. Energy deposition into the gas are calculated thanks to the f8 tally of MCNP6 code, and compared to pulse height spectra acquired experimentally. Fig. 3 and Fig. 4 show respectively spectra from 65NH45 counter and from CPNB48 counter. In Fig. 3, the observed peak at 764 keV comes from the full deposition of both the proton and the triton. In Fig. 4, the shape of the spectrum comes from the self-absorption phenomenon into the deposit where the cliff at 1.47 MeV corresponds to the full deposition of the alpha particle, and the cliff at 840 keV corresponds to the full deposition of the lithium ion. Experimental spectra (in voltage) are calibrated in energy matching them with simulated ones.

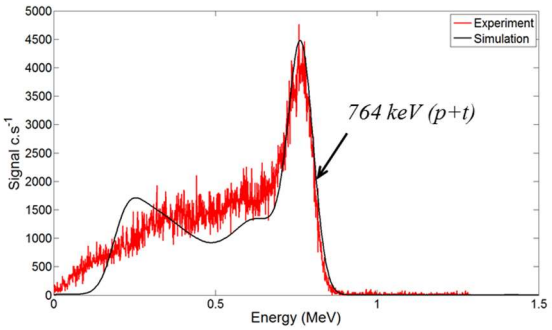

Fig. 3. Experimental and simulated spectra obtained with 65NH45.

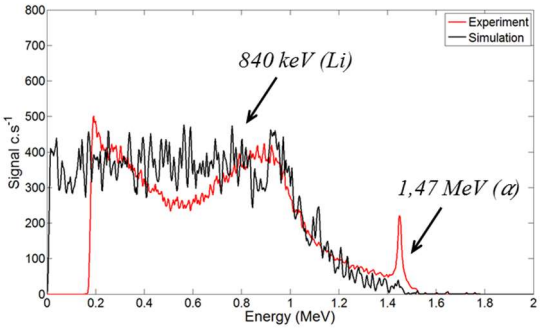

Fig. 4. Experimental and simulated spectra obtained with CPNB48.

The estimated count rate $\hat{S}$ is calculated by integration of the pulse height tally $Y(E)$ estimated by MCNP6 where E_m is the energy threshold, A_{Cf} is the activity of the ^{252}Cf source, η_f is the number of fission per ^{252}Cf disintegration, ν_n is the number of neutron per fission, and t is the measurement time such as:

$$\hat{S} = \frac{\eta_f \nu_n A_{Cf}}{t} \int_{E_m}^{\infty} Y(E)dE \qquad (1)$$

The threshold E_m is adjusted in order to match simulated count rate profiles with experimental ones. Fig. 5 and Fig. 6 presents count rate profiles obtained for respectively 65NH45 and CPNB48 counters.

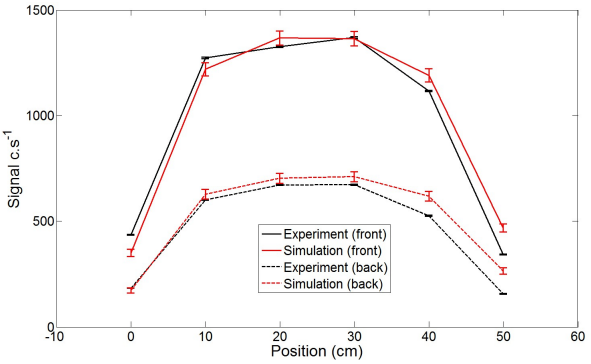

Fig. 5. Experimental and simulated profiles obtained with 65NH45.

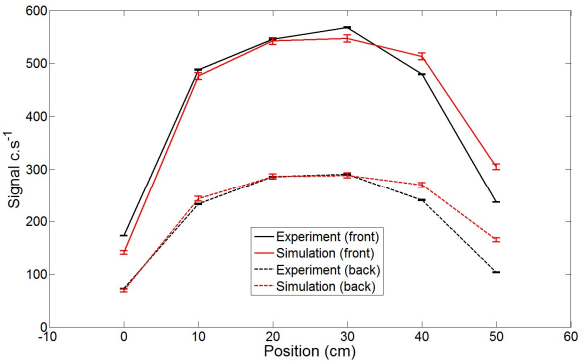

Fig. 6. Experimental and simulated profiles obtained with CPNB48.

This absolute calibration allows us to estimate the quantity of events lost into the deposit (if any) and the quantity lost by discrimination. Table 1 displays the results obtained by this calibration study.

Table 1. Calibration of counter model.

	65NH45	CPNB48	CFUC07
Threshold E_m	175 keV	450 keV	?
Loss in deposit	0 %	23 %	?
Loss in discrimination	32 %	10 %	?
Total loss	32 ± 1 %	33 ± 1 %	35 ± 1 %

V. GAMMA RAY SHIELDING

The activation product source term has been estimated by activation calculation under nominal condition [26]. Following activities have been estimated:

- 310 GBq.kg^{-1} for the ^{24}Na,
- 37 MBq.kg^{-1} for the ^{22}Na,
- 170 GBq.kg^{-1} for the ^{23}Ne,
- 250 GBq.kg^{-1} for the ^{20}F.

The corresponding emission spectrum is displayed in Fig. 7.

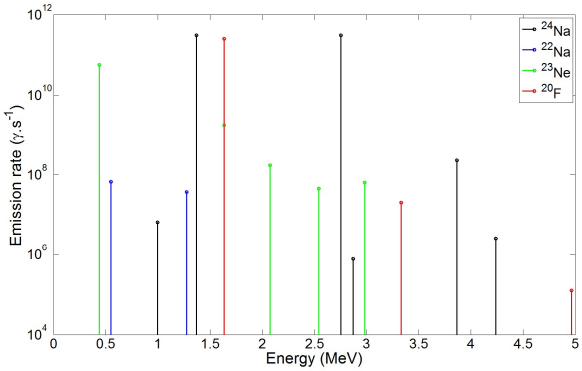

Fig. 7. Gamma ray emission spectrum of the sodium source.

Gamma rays can impact the neutron measurement in two manners: inducing pile-up pulses in detectors and producing photoneutron.

A. *Gamma ray pile-up management*

The shield against gamma rays controls the dose rate impinging neutrons detectors. The dose rate at the outlet of the shield is estimated using a flux point tally (F5) weighted by a transfer function provided by the ICRP87 [27]. Fig. 8 shows the dose rate evolution as a function of the shield thickness in the case of lead and in the case of tungsten. Linear attenuation coefficients have been estimated to values equal to 0.554±0.006 cm^{-1} for the lead and 0.65±0.05 cm^{-1} for the tungsten.

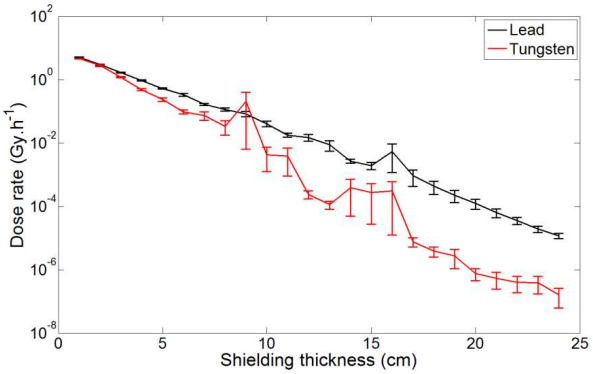

Fig. 8. Dose rate around the shied as a function of its thickness (MCNP6 calculation).

The gamma rays pile-up can have a significant impact on signal (false count rate). The discrimination threshold has to be set in regards with the maximal incident gamma dose rate of the experiment in order to avoid any false neutron events. In quid pro quo, the neutron sensitivity will decrease as a function of the threshold magnitude. Implementing the optimal concentration of quenchers into the gas mix and coupling the detector with a high bandgap preamplifier will give us all the chance to limit the count rate loss for a given gamma dose rate. According to literature and recent measurements, a limit count rate loss below 30 % compared to the ambient dose rate configuration, permits to operate up to 1 $Gy.h^{-1}$ with ^{3}He counters and up to 10 $Gy.h^{-1}$ with ^{10}B counters [28-29]. Fig. 9 displays values of counting loss as a function of the gamma dose rate obtained using an intensive ^{137}Cs source. Fission ion chambers are particular cases in which no loss is observed below 100 $Gy.h^{-1}$ due to the very high Q-value of the fission reaction.

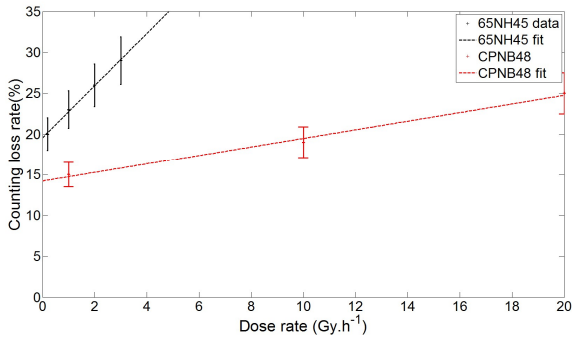

Fig. 9. Experimental and simulated profiles obtained with CPNB48.

To comply with the requirement to protect neutron detection from pile-up induced false events while maintaining good detection efficiency, a minimal shield thickness is proposed in Table 2 for each configuration (a large security margin has been taken into account).

Table 2. Estimation of the shield thickness against gamma pile-up phenomenon.

	65NH45	CPNB48	CFUC07
Dose rate limit	1 $Gy.h^{-1}$	10 $Gy.h^{-1}$	>100 $Gy.h^{-1}$
Pb thickness	5 cm	1 cm	0 cm
W thickness	4 cm	1 cm	0 cm
Loss at low dose rate	32 %	33 %	35 %
Loss at high dose rate*	30 %	30 %	0 %

* Relatively to count rate values at low count rate.

It can be observed that tungsten provides a better gamma rays stopping power than lead, but tungsten has a dramatically lower neutron transparency ($\sigma_{W(n,\gamma)}$=18.3 b compared with $\sigma_{Pb(n,\gamma)}$=175 mb). The slight gamma shielding gain achieved with tungsten will dramatically penalize the neutron sensitivity. Only the lead shield will be therefore considered in the following of the study.

B. *Photoneutron management*

Photoneutrons can be produced by (γ,n) reactions on deuterium isotopes contained in polyethylene. The photonuclear threshold of this reaction is equal to 2.23 MeV which is below the highest intensive quantum emission of ^{24}Na at 2.754 MeV [30]. Fig. 10 shows the $^{2}H(\gamma,n)$ cross-section as a function of the incident energy of gamma rays.

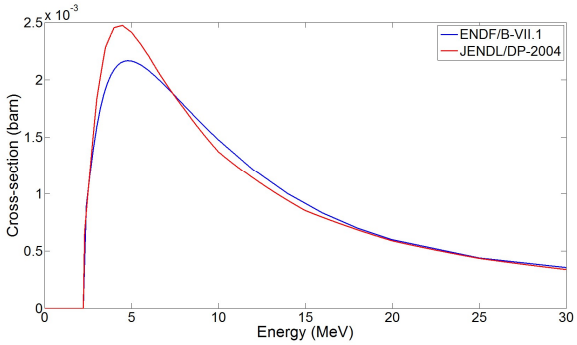

Fig. 10. Cross-section of the reaction $^{2}H(\gamma,n)$ extracted from ENDF/B-VII.1 and JENDL/DP-2004 data bases.

An ^{3}He counter is set into polyethylene moderator surrounding the lead shield with an external diameter equal to 70 cm. The detector response to photoneutron as a function of the lead thickness is estimated by MCNP6 calculation. Neutron scatterings in polyethylene are led by S(α,β) library ENDF71SaB and photo-atomic data comes from ENDF/B7.0 libraries [31,32]. As observed in Fig. 11, the photoneutron signal is equal to 446 cps without any shield and falls dramatically under 1 cps with a lead

thickness equal to 12 cm thanks to the mutual attenuation and smoothering effect of the lead on the photon flux.

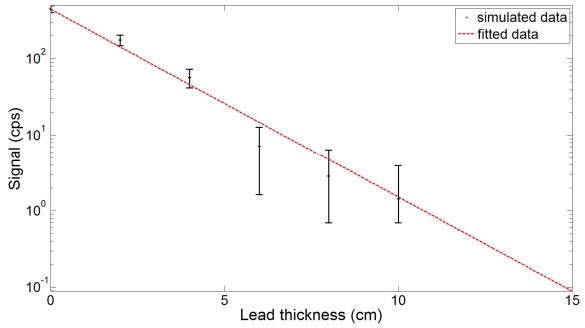

Fig. 11. Photoneutron signal of 65NH45 ^{3}He counter as a function of the thickness of the lead shielding.

The use of polyethylene imposes the implementation of a lead shields with a thickness equal to 12 cm. Thus, the photoneutron signal falls in the range of magnitude of the signal from cladding external pollution. As predicted, no photoneutron signal is measured with graphite moderator.

VI. MAXIMIZATION OF THE SIGNAL FROM FISSION PRODUCTS

Delayed neutron precursors can be classified in 8 groups of decay periods such as presented in the Table 3.

Table 3. List of delayed neutron precursors classified per group of decay period.

Group	Precursor	Decay period (s)
1	^{87}Br	55.65
2	^{137}I	24.50
3	^{88}Br	16.31
4	^{138}I, ^{93}Rb, ^{89}Br	6.47, 5.86, 4.53
5	^{94}Rb, ^{139}I, ^{85}As, ^{98m}Y	2.71, 2.28, 2.03, 2.00
6	^{93}Kr, ^{144}Cs, ^{140}I	1.29, 1.00, 0.86
7	^{91}Br, ^{95}Rb	0.541, 0.378
8	^{96}Rb, ^{97}Rb	0.203, 0.169

The transit from sampling point (assembly outlet or intermediate heat exchangers) to the measurement volume is comprised between 15 and 30 s. We can therefore focus the study on first groups of fission products: ^{87}Br, ^{137}I, ^{88}Br, where neutrons are emitted in the range comprised between 20 keV and 1.4 MeV as presented in Fig. 12.

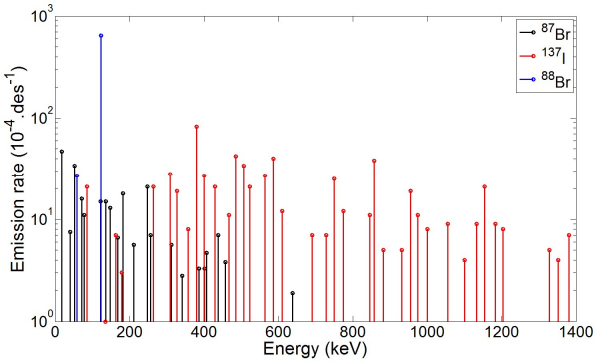

Fig. 12. Discrete delayed neutron emission from ^{87}Br, ^{137}I, ^{88}Br extracted from JEFF-3.1.1 library.

Let consider 6 configurations such as:

- 12 cm of lead shied and polyethylene moderator with,
  - 65NH45, CPNB48, or CFUC07 detectors,
- 5 cm of lead shield and graphite moderator with 65NH45 counter,
- 1 cm of lead shield and graphite moderator with CPNB48 counter,
- No lead shield and graphite moderator with CFUC07 chamber.

The neutron sensitivity is estimated according to the experimental calibration for different position of detector into the moderator. Fig. 13 and Fig. 14 present sensitivity estimations in respectively polyethylene and graphite configuration. It can be observed that the ^{3}He proportional counter provides sensitivity 3 times higher that ^{10}B proportional counter and 30 times higher that fission chamber. The loss of moderating ability when graphite is used instead of polyethylene is fully compensated by the neutron-source distance reduction allowed by the removal of photoneutron specific shield. Although this effect is more contrasted in the case of polyethylene moderator, the sensitivity is maximized when detectors are located in the most internal part of the moderator. Results maximizing sensitivity to delayed neutron are summarized in Table 4.

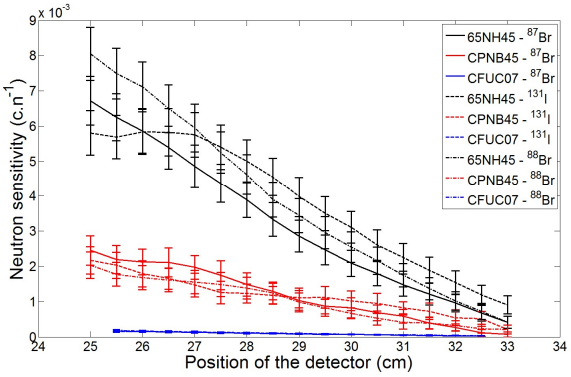

Fig. 13. Neutron sensitivity of detector as a function of the detector location in the polyethylene moderator. The distance is taken from the sodium volume axis to the detector axis.

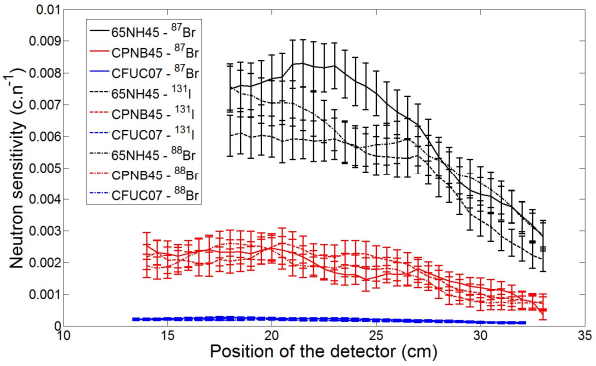

Fig. 14. Neutron sensitivity of detector as a function of the detector location in the graphite moderator. The distance is taken from the sodium volume axis to the detector axis.

Table 4. Estimations of the sensitivity per detector.

	Polyethylene	Graphite
Lead thickness	12 cm for all	5 cm, 1 cm, 0 cm*
Photoneutrons signal	< 1cps	0 cps
Delayed neutron sensitivity 65NH45	$(7.0\pm1.8).10^{-3}$ c.n^{-1}	$(6.9\pm1.4).10^{-3}$ c.n^{-1}
Delayed neutron sensitivity CPNB48	$(2.3\pm0.6).10^{-3}$ c.n^{-1}	$(2.2\pm0.7).10^{-3}$ c.n^{-1}
Delayed neutron sensitivity CFUC07	$(1.7\pm0.4).10^{-4}$ c.n^{-1}	$(2.1\pm0.3).10^{-4}$ c.n^{-1}

* For respectively 65NH45, CPNB48, and CFUC07

The delayed neutron source term has been calculated (Grenadine code) for a clad failure equal to 1 cm².R using a recoil model as described in [33-34]. Rough estimation of absolute sensitivities gives:

- 60 cps per cm².R per 65NH45 counters,
- 20 cps per cm².R per CPNB48 counters,
- 1.5 cps per cm².R per CFUC07 fission chambers.

This results have to be compared with the pollution signal which can be considered in 1 to 3 cps in the configuration based on polyethylene and 65NH45 counters (quite similar to Superphenix one) [35]. The shutdown of the reactor is typically trigged according with two conditions:

- The delayed neutron signal overtakes a threshold corresponding to 25 cm².R,
- Or the differential delayed neutron signal overtakes 4 cm².R.min^{-1}.

We have therefore all reason to trust in proposed ex-vessel DND systems to address this safety issues with a convenient response time.

VII. Limitation of the External Dose Rate

The dose rates in operation around the DND system have been estimated using the same method as in chap. V.A and reported in Table 5 for different distance from the system. The diminution or the suppression of the internal shielding in graphite configuration induces an increase of the external dose rate up to a factor 10. If needed, an external shield can be added to compensate this effect in regards to radioprotection requirement. Dose rate estimations where an external tungsten shield with a thickness equal to 5 cm are displayed in Table 6. The external dose rate is divided by 30 while keeping an acceptable neutron sensitivity reduction below 25 %.

Table 5. Estimations of the dose rate in mSv.h^{-1} around the system.

	Contact	50 cm	1 m
CH_2	11±3	2.4±0.2	1.0±0.1
C + ^{3}He	290±60	27±1	11.1±0.6
C + ^{10}B	1250±100	120±3	48.5±1
C + CFU	2200±150	185±4	73±1

Table 6. Estimations of the dose rate in mSv.h^{-1} around the system where 5 cm of tungsten is added as an external shielding.

Conf.	Contact	50 cm	1 m	Sensitivity loss
CH_2	14±8	0.07±0.02	0.03±0.008	-4.17%
C + ^{3}He	120±35	0.9±0.15	0.3±0.05	-25.3%
C + ^{10}B	638±100	4.2±0.4	1.7±0.2	-5.56%
C + CF	850±180	6.3±0.5	2.6±0.2	-22.7%

Fig. 15 shows as an illustration, the schematic of DND system using graphite moderator and implemented 3 ^{3}He counters allowing operating in 2/3 rules of detection.

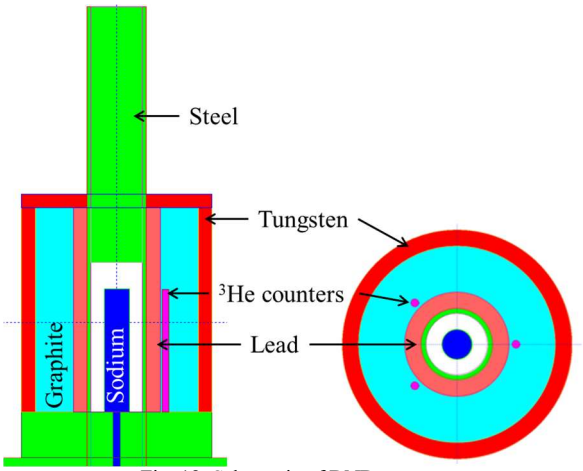

Fig. 12. Schematic of DND system.

VIII. Conclusion

Ex-vessel DND systems have been studied to address safety solutions in the framework of the ASTRID project. Base on state-of-the-art, a simulation study has been conducted in order to improve the understanding about physical phenomena governing the delayed neutron measurement.

It has been highlighted that the impact of gamma pulse pile-up can be easily managed under the moderate dose rate emitted by activation products, whereas the impact of photoneutrons produced in polyethylene moderator requires a lead thickness up to 12 cm to fall under 1 cps. Graphite moderator can be an alternative offering a complete suppression of photoneutron while maintaining suitable neutron sensitivity.

^{3}He proportional counter provides the best detection sensitivity. They can be replaced by ^{10}B proportional counters with a 3 times lower sensitivity and by fission with a 30 times lower sensitivity.

The external dose rate can be adjusted and falls below 10 mSv.h^{-1} thanks an additional external tungsten shield.

REFERENCES

[1] B.W. Brook, A. Alonso, D.A. Meneley, *et al*., "Why nuclear energy is sustainable and has to be part of the energy mix", *Sustainable Materials and Technologies*, vol. 1–2 pp. 8-16, 2014.

[2] GENIV International Forum,"Technology roadmap update for generation IV nuclear energy systems", *OECD NEA report*, 2014.

[3] S. Pivet, "Status of the French Fast Reactor Program", *In proceedings of IAEA FR17 Fast Reactors and Related Fuel Cycles conference*, 2017.

[4] R. Coulon, S. Normand, G. Ban, *et al*., "Delayed gamma power measurement for sodium-cooled fast reactors", *Nuclear Engineering and Design* 241, pp. 339–348, 2011.

[5] R. Rohée, "Cladding failure detection for sodium cooled fast reactor using high count rate gamma spectrometry", *Ph.D. Thesis of the University of Caen Normandy*, 2016.

[6] R. Coulon, E. Rohée, S. Garti, *et al.*, "Detection and analysis of fuel cladding damages using gamma ray spectrometry", *In proceedings of IAEA FR17 Fast Reactors and Related Fuel Cycles conference*, 2017.

[7] D.-T. Costin, L. Desgranges, T. Retegan, C. Ekberg, "Storage of defective fuel pins in SFR core", *Procedia Chemistry* 21, pp. 378-385, 2016.

[8] B.J. Lewis, P.K. Chan, A. El-Jaby, *et al*., "Fission product release modelling for application of fuel-failure monitoring and detection - An overview", *Journal of Nuclear Materials,* vol. 489, pp. 64-83, 2017.

[9] D.B. Sangodkar, "Failed fuel element detection and location in fast breeder test reactor", *In proceedings of IAEA Fuel Failure Detection and Location in LMFBRs Meeting*, pp. 53-59, 1982.

[10] F.S. Kirn, J.D.B. Lambert, F.E. Holt, *et al*., "Fuel failure monitoring systems in U.S. breeder reactors", *In proceedings of IAEA Fuel Failure Detection and Location in LMFBRs Meeting*, pp. 75-81, 1982.

[11] S. Sekiguchi, R. Rindo, T. Miyazawa, "Failed fuel detection and location system in the Japanese LMFBRs", *In proceedings of IAEA Fuel Failure Detection and Location in LMFBRs Meeting*, pp. 60-66, 1982.

[12] C. Berlin, "Evolution of FFD-FFL instrumentation on French fast reactors", *In proceedings of IAEA Fuel Failure Detection and Location in LMFBRs Meeting*, pp. 36-44, 1982.

[13] S. Ukai, I. Shibahara, Y. Enokido, *et al*., "Release characterization of delayed neutron precursors from breached FBR fuel element", *Journal of Nuclear Science and Technology*, vol. 26, pp. 931-938, 1989.

[14] C. Berlin, "Localization of the first clad failure", *In proceedings of IAEA Fuel Failure Detection and Location in LMFBRs Meeting*, pp. 11,141, 1982.

[15] O.I. Albutova, D.A. Lukyanov, "Investigation of dependence of BN-600 reactor sector fuel cladding leak detection system responses on the operation parameters", *Nuclear Energy and Technology*, vol.1, pp. 248-252, 2015.

[16] D.A. Lukyanov, P. Dvornikov, A. Staroverov, *et al*. "Experience of commissioning of the sectoral monitoring tightness system of fuel elements claddings (SSKGO) of RF BN-600, RF BN-800", *In proceedings of IAEA FR17 Fast Reactors and Related Fuel Cycles conference*, 2017.

[17] P. Filliatre, C. Jammes, N. Chapoutier, *et al*., "In vessel detection of delayed neutron emitters from clad failure in sodium cooled nuclear reactors: An estimation of the signal", *Nuclear Instruments and Methods* A, vol. 744, pp. 1-10, 2014.

[18] E. Rohée, R. Coulon, C. Jammes, P. Filliatre, *et al*., "Delayed Neutron Detection with graphite moderator for clad failure detection in Sodium-Cooled Fast Reactors", *Annals of Nuclear Energy*, vol. 92, pp. 440-446, 2016.

[19] P. Filliatre, C. Jammes, J.-P. Jeannot, F. Jadot, "In vessel detection of delayed neutron emitters from clad failure in sodium cooled nuclear reactors: Information treatment", *Annals of Nuclear Energy*, vol. 65, pp. 385-389, 2014.

[20] R. Coulon, J. Dumazert, V. Kondrasovs, S. Normand, "Implementation of a nonlinear filter for online nuclear counting", *Radiation Measurements*, 87, pp. 13-23, 2016.

[21] R. Coulon, V. Kondrasovs, J. Dumazert, *et al*., "Estimation of Nuclear Counting by a Nonlinear Filter Based on a Hypothesis Test and a Double Exponential Smoothing" *IEEE Transactions on Nuclear Science*, vol. 63, no. 5, pp. 2671-2676, 2016.

[22] C.H. Lee, H.S. Kim, J.H. Ha, *et al*., "Characteristics of Fabricated SiC Radiation detectors for fast neutron detection", *Journal of Radiation Protection*, vol. 37, n°2, pp. 70-74, 2012.

[23] F. Foulon, P. Bergonzo, V.N. Amosov, *et al*., " Characterization of CVD diamond detectors used for fast neutron flux monitoring", *Nuclear Instruments and Methods A*, vol. 476, pp. 495-499, 2002.

[24] J. Dumazert, R. Coulon, V. Kondrasovs, Karim Boudergui, "Compensation scheme for online neutron detection using a Gd-covered CdZnTe sensor", *Nuclear Instruments and Methods A*, vol. 857, pp. 7-15, 2017.

[25] "MCNP6 User's Manual Version 1.0". *LANL Technical Report LA-CP-13-00634*, chap. 3, pp. 71-72, 2011.

[26] C. Kocher, N. Chapoutier, "Neutron and thermal hydraulic conditions for core instrumentation", *AREVA NT technical report* PEPL-F 2011 DC 79 C, 2012.

[27] ICRP, 1987. Data for Use in Protection against External Radiation. ICRP Publication 51. Ann. ICRP 17 (2-3).

[28] T. Domenech, "Impact of gamma rays on thermal neutron sensitivity of proportional counters", *CEA Technical Report*, DRT/LIST/DCSI/RAP/10-0474, 2010.

[29] D.H. Beddingfild, N.H. Johnson, H.O. Menlove, "^{3}He neutron proportional counter performance in high gamma-ray dose environments", *Nuclear Instruments and Methods A*, vol. 455, pp. 670-682, 2000.

[30] R.C. Mobley, R.A. Laubenstein, "Photo-neutron thresholds of beryllium and deuterium", Physical review, vol. 80, n° 3, pp. 309-315, 1950.

[31] D.K. Parsons, J.L. Conlin, "Release of continuous representation for S(α,β) ACE data", *LANL Technical Report LA-UR-14-21878*, 2014.

[32] M.C. White, R.C. Little, M.B. Chadwick, "Photonuclear Physics in MCNP(X)". *Proceedings of the ANS meeting on Nuclear Applications of Accelerator Technology,* 1999.

[33] B. Majournat, "Optimization of the failed fuel location system", *Novatome Technical Report,* C2 06 51312, 1992.

[34] B.J. Lewis, P.K. Chan, A. El-Jaby, *et al*., "Fission product release modelling for application of fuel-failure

monitoring and detection - An overview", *Journal of Nuclear Materials*, vol. 489, pp. 64-83, 2017.
[35] J-P. Trapp. "Cladding failures in sodium cooled fast reactors – Phenomenology and detection in reactors ". *CEA Technical Report*, LSMN/2000/0001, 2000.